Mehran University Research Journal of Engineering and Technology

https://doi.org/10.22581/muet1982.0678

2026, 45(3) 124-131

A Finite Element Simulation for the Analysis of Ball Bearing Contact and Fatigue Using Goodman Theory

Saima Bhatti [1*], Asif Mansoor [2], Obaidullah Khan [3], Asif Ali Shaikh [1]

[1] *Department of Basic Science and Related Studies, Mehran University of Engineering and Technology, Jamshoro 76062, Pakistan*

[2] *Department of Industrial and Manufacturing Engineering, Pakistan Navy Engineering College, National University of Sciences and Technology, Karachi 07548, Pakistan*

[3] *Department of Naval Architecture, Platform Design House, Pakistan Navy Engineering College, Karachi 07548, Pakistan*

[*] Corresponding author: saima.bhatti@faculty.muet.edu.pk

Received: 24 December 2025, Revised: 14 June 2026, Accepted: 22 June 2026, Published: 01 July 2026

KEYWORDS

Rolling Bearings
Finite Element Method
Fatigue Life
Contact Analysis
Stress Distribution

ABSTRACT

Ensuring the mechanical integrity and service life of rolling-element bearings requires a clear understanding of contact stresses under operational loading. This study presents a finite element analysis of a deep-groove ball bearing in ANSYS, where the load is transferred from the shaft through the rolling elements to the outer race. The Goodman and Soderberg mean-stress criteria were integrated with the contact model to compare fatigue predictions. A mesh-independence study used 10,000, 25,000, and 70,000 elements. At a radial pressure of 100 MPa, the maximum von Mises stress was approximately 496 MPa, and local factor-of-safety values were below 1.0, indicating a risk of local yielding and premature fatigue failure. Reducing the pressure to 10 MPa increased the minimum Goodman factor of safety to 1.73 and extended the predicted fatigue life to 1×10^6 cycles. The Soderberg criterion consistently produced lower safety factors and shorter life estimates than the Goodman criterion under the same loading conditions. The integrated framework generates spatially resolved stress, safety-factor, and fatigue-life maps that can support bearing-design optimisation and predictive maintenance of rotating machinery.

1. Introduction

Rolling-element bearings are fundamental mechanical components that support radial and axial loads while reducing friction, thereby improving the efficiency and reliability of rotating machinery [1–3]. The interactions between rolling elements and raceways are central to bearing performance analysis because they directly affect load distribution, stress concentrations, wear, and service life. Classical Hertzian contact theory provides closed-form solutions for contact stresses under idealised assumptions, including perfectly elastic, smooth, homogeneous bodies and nonconforming contact surfaces. Actual bearings, however, operate under non-ideal conditions. Elastohydrodynamic lubrication separates contacting surfaces at high pressure and speed, thereby reducing friction and wear. Temperature variations alter material properties and lubricant behaviour, while misalignment and time-varying loads further complicate the system response [4,5].

These departures from ideal Hertzian conditions require advanced modelling approaches for accurate prediction of contact-pressure distributions, subsurface stress fields, including orthogonal shear stress, and the onset of plastic deformation. The finite element method (FEM) has therefore become an effective numerical tool for high-fidelity simulation of complex contact behaviour. State-of-the-art FEM

© Mehran University of Engineering and Technology 2026

analyses can incorporate material nonlinearity, realistic geometry, contact interactions, and dynamic loading to provide detailed insight into load sharing, deformation at high rotational speeds, and the initiation of failure mechanisms [6–8].

Accurate contact modelling is essential for prognostic health management and service-life prediction of rolling-element bearings. Small differences in contact assumptions can substantially affect stress distributions and fatigue-life estimates. In modern maintenance practice, component monitoring enables early detection of potential failures, improves machine health, reduces downtime, and enhances operational safety [9]. Such a prediction is particularly important in high-speed rotating machinery, where bearing failure can cause severe system-level consequences.

Recent advances in engineering software, including ANSYS and SolidWorks Simulation, have enabled realistic modelling of complex mechanical systems. These tools can represent detailed geometries, validated material properties, contact definitions, and operating conditions with high numerical precision [10,11]. Established analytical approaches, such as the bearing stiffness-matrix method developed by Guo and Parker [12] and the design procedures reported by Harris and Kotzalas [13], also provide important foundations for bearing analysis.

Traditional fatigue assessment under cyclic loading commonly considers the combined effects of mean and alternating stresses; the Goodman relation remains widely used for this purpose [14]. Integrating high-fidelity numerical simulation with established analytical and empirical fatigue criteria enables a more comprehensive assessment of bearing performance and service life.

2. Finite Element Simulation and Goodman Fatigue Theory

The primary objective of this study is to evaluate the contact stresses and fatigue behaviour of a deep-groove ball bearing using finite element simulation and Goodman mean-stress theory. Bearings in rotating machinery experience combinations of static and cyclic loading; accurate fatigue-life prediction is therefore essential for reliability, safety, and efficient operation. A systematic FEM framework was developed by combining static structural analysis with a fatigue-reliability assessment based on the Goodman criterion.

The finite element model represents realistic contact conditions, material behaviour, and load transfer within the bearing assembly. It provides detailed stress fields, particularly in the critical contact regions where fatigue cracks are most likely to initiate. The static structural results are subsequently used to calculate mean and alternating stresses for the Goodman fatigue assessment.

By integrating numerical simulation with classical fatigue theory, the proposed methodology provides a systematic procedure for predicting bearing life. The resulting stress and safety-factor maps support improved design, maintenance planning, and long-term reliability.

2.1 Goodman Fatigue Relation

Fatigue failure can occur in mechanical components subjected to fluctuating stresses. The Goodman criterion is an empirical method for evaluating component safety under such conditions while accounting for the detrimental effect of mean stress. The Goodman relation is expressed as:

$$\frac{\sigma_a+\sigma_e}{\sigma_m+\sigma_u} \leq 1 \quad (1)$$

In Eq. (1), the endurance limit is denoted by σu, the ultimate tensile strength by , the alternating stress by σ_a, and the mean stress by σ_m. Eq. (2) defines the factor of safety (FOS) as :

$$FOS = \frac{1}{\frac{\sigma_a+\sigma_e}{\sigma_m+\sigma_u}} \quad (2)$$

The alternating and mean stresses are derived from the maximum and minimum stress values in a load cycle:

$$\sigma_a = \frac{\sigma_{max}-\sigma_{min}}{2} \quad (3)$$

$$\sigma_m = \frac{\sigma_{max}+\sigma_{min}}{2} \quad (4)$$

2.2 Finite Element Simulation Algorithm

The Goodman relation was evaluated at the element level within the finite element model to obtain a spatially resolved fatigue assessment.

Step 1: Material properties and model setup

Structural steel was selected as the bearing material. The FEM simulation was configured in ANSYS Mechanical 2021 R2 using the Static Structural module. A three-dimensional model of the deep-groove ball bearing was created, and contact interactions between the balls and the inner and outer

© Mehran University of Engineering and Technology 2026

rings were defined to ensure realistic load transfer (Fig. 2).

Step 2: Mesh independence and boundary conditions

A mesh-independence study was performed using coarse (10,000 elements), medium (25,000 elements), and fine (70,000 elements) meshes, as shown in Figs. 3(a)–(c). The fine mesh, which had a maximum skewness of 0.95, was selected for the subsequent analyses. Mesh-quality distributions are presented in Figs. 4 and 5. The outer ring was fixed, and radial pressure was applied to the inner ring through the shaft, as illustrated in Figs. 6 and 7.

Step 3: Stress computation and FOS evaluation

A static structural model (SSM) was solved for two extreme load cases to obtain σ_{max} and σ_{min} at each element i. Eqs. (3) and (4) were used to calculate $\sigma_a^{(i)}$ and $\sigma_m^{(i)}$. The factor of safety of each element was then determined using Eq. (2), enabling direct identification of critical regions where FOS < 1.

3. Simulation Setup in ANSYS Mechanical

Numerical analysis was conducted using the static structural model in ANSYS Mechanical 2021 R2. Structural steel was assigned to the bearing components, and contact interactions between the balls and the inner and outer rings were defined to represent load transfer. Each ball was modelled in contact with both rings, as shown in Fig. 2.

Fig. 1 summarises the structural and fatigue properties of the bearing material, including a Young's modulus of 200 GPa, Poisson's ratio of 0.30, an ultimate tensile strength of 460 MPa, and a yield strength of 250 MPa.

The fatigue data show that stress and strain amplitudes decrease as the number of cycles increases from 10^3 to 10^6, indicating longer fatigue life at lower loading levels.

A mesh-independence study was conducted using three mesh densities: coarse (10,000 elements), medium (25,000 elements), and fine (70,000 elements), as shown in Figs. 3(a)–(c). The maximum skewness of the fine mesh was 0.95, below the adopted critical limit of 0.99. The skewness and aspect-ratio distributions in Figs. 4 and 5 further demonstrate the adequacy of the selected mesh for the subsequent simulations.

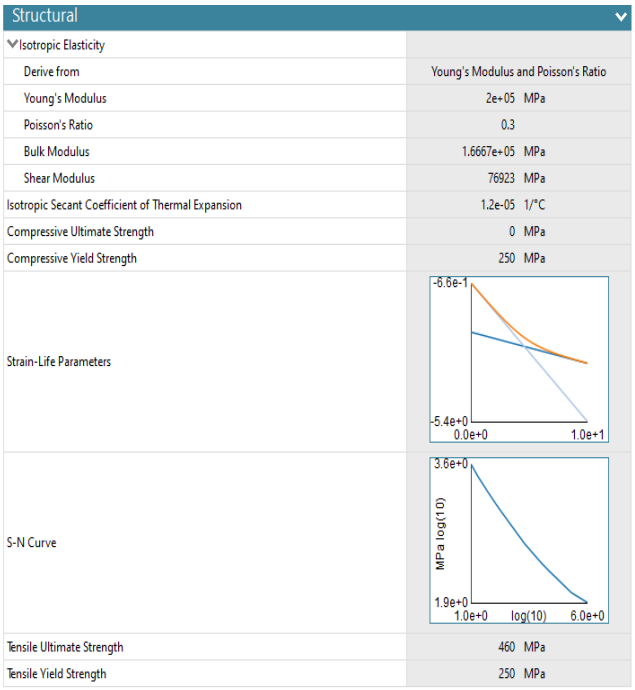

Fig. 1. Mechanical Properties of a Ball Bearing

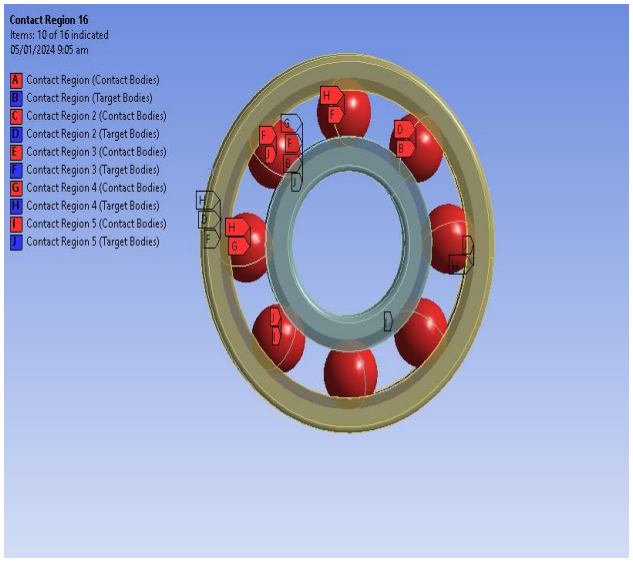

Fig. 2. Contact Regions Between Balls and Rings

This arrangement represents load transfer through the rolling elements to the stationary outer ring.

The outer surface of the outer ring was fully constrained. Radial-pressure cases of 100 MPa and 10 MPa were applied to the inner ring through the shaft for the comparative fatigue analyses (Figs. 6 and 7).

Fig. 6 shows the boundary conditions of the bearing model: the outer ring is fully constrained, and pressure is applied to the inner race. This setup simulates load transfer through the rolling elements to the stationary outer ring.

© Mehran University of Engineering and Technology 2026

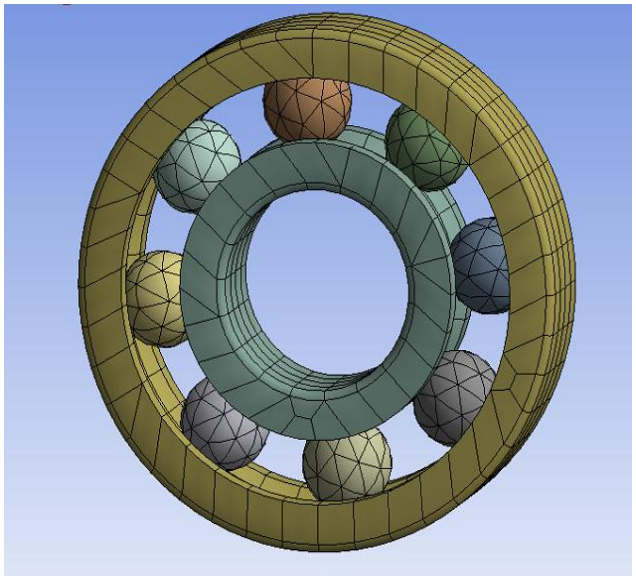

Fig. 3(a). Coarse Mesh of the Ball Bearing (10,000 Elements)

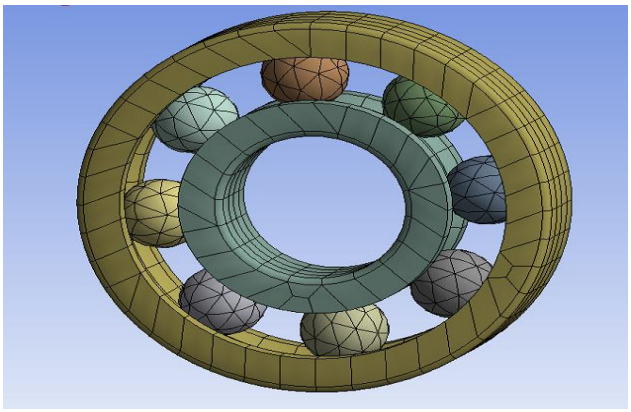

Fig. 3(b). Medium Mesh of the Ball Bearing (25,000 Elements)

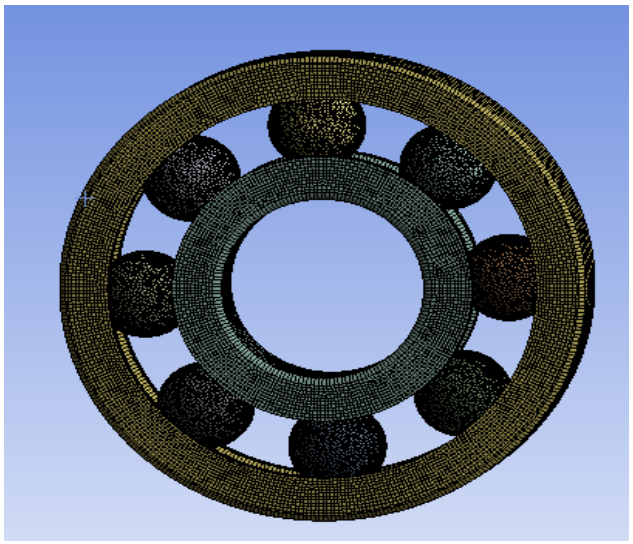

Fig. 3(c). Fine Mesh of the Ball Bearing (70,000 Elements)

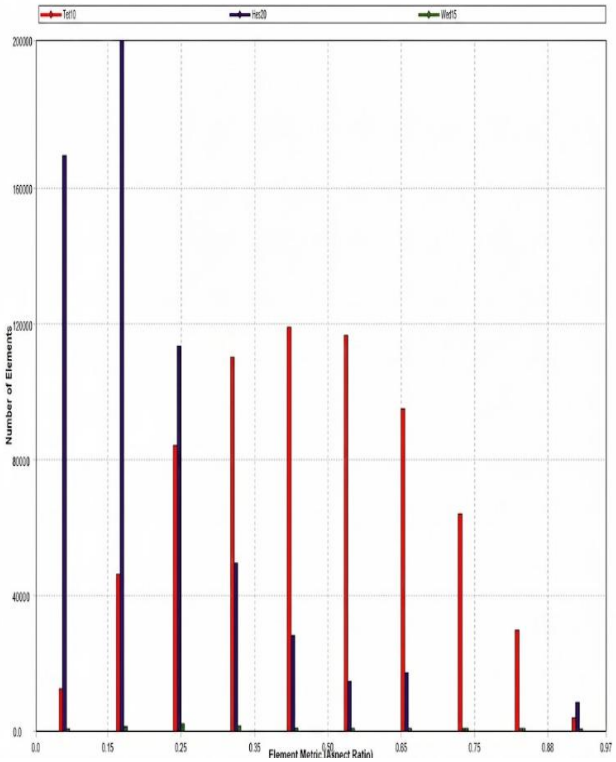

Fig. 4. Fine-Mesh Skewness of the Ball Bearing

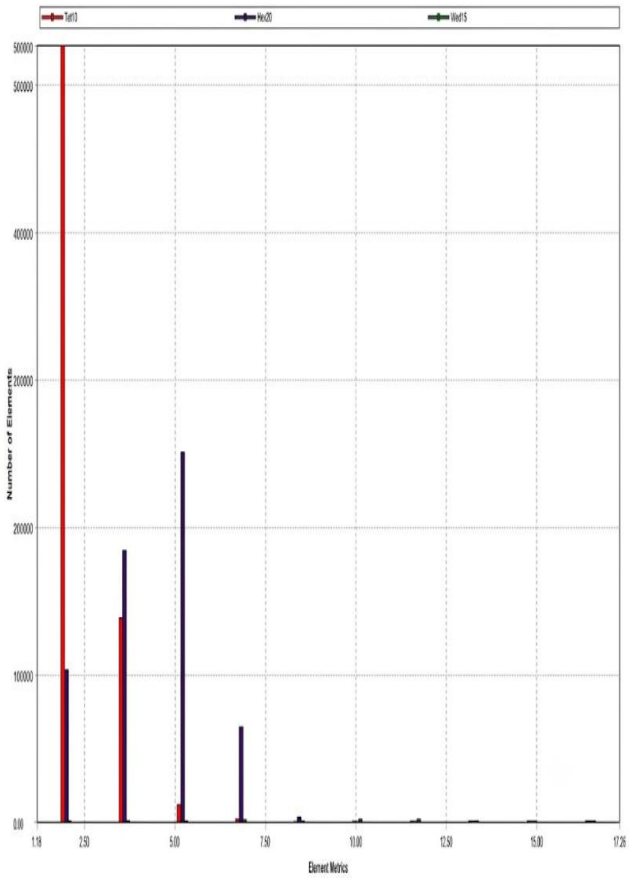

Fig. 5. Fine-Mesh Aspect Ratio of the Ball Bearing

© Mehran University of Engineering and Technology 2026

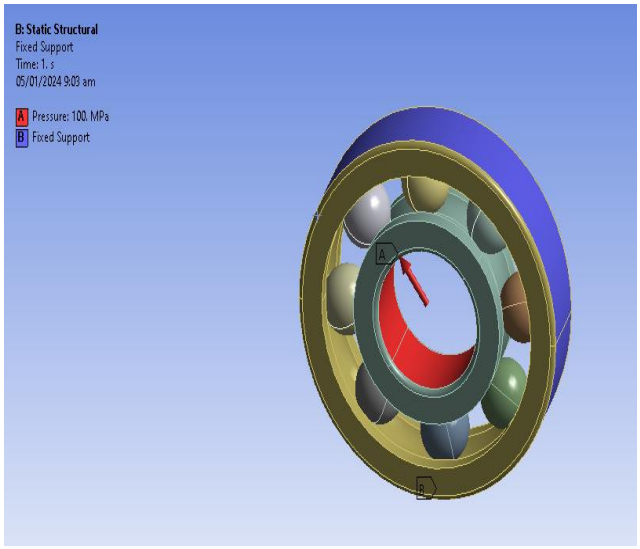

Fig. 6. Boundary Conditions for Static Analysis of the Ball Bearing

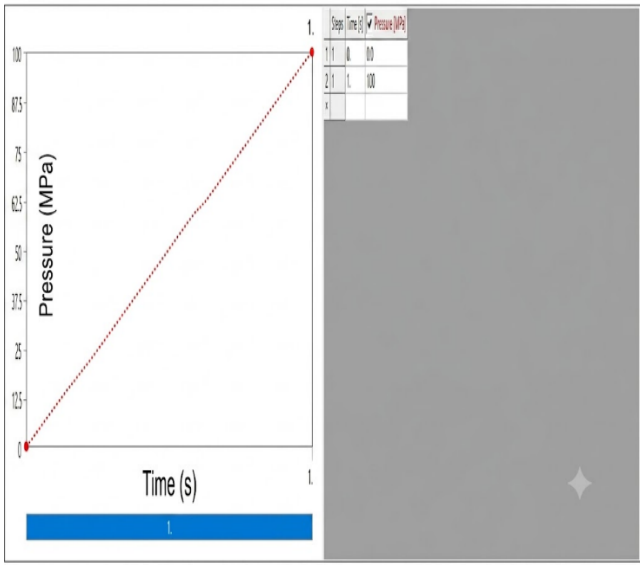

Fig. 7. Applied Radial Pressure

Fig. 7 shows the linearly ramped radial pressure used in the static analysis. The linear load history is consistent with the elastic formulation of the model. Realistic constraints and a refined mesh were used to improve solution accuracy and convergence, particularly in regions with steep stress gradients.

ANSYS solved the model under the prescribed constraints to obtain displacement, stress, and strain distributions. The stable solution and mesh-quality assessment support the use of these numerical results in the subsequent contact and fatigue analyses.

4. Results and Discussion

The results describe the contact-stress distribution, fatigue response, and predicted life of the rolling-element bearing under the prescribed loading conditions. Particular attention is given to the ball–race contact interfaces, where stress concentrations are highest and fatigue damage is most likely to initiate. The analysis also clarifies how mechanical loads are transmitted through the bearing components and how they influence the local stress field.

The bearing response to cyclic loading was also evaluated to identify potential failure zones and assess fatigue performance over repeated load cycles. The time variation of stress was used to examine the initiation and progression of fatigue damage.

Service life was estimated using fatigue-life models that account for contact stress, material properties, and loading history. These results identify the parameters governing bearing reliability and durability and can inform bearing design, maintenance planning, and prognostic health-management applications for rotating machinery.

4.1 Contact Stress Analysis

The finite element solution provided detailed distributions of von Mises equivalent stress and elastic strain. At a radial pressure of 100 MPa, the maximum von Mises stress was approximately 496 MPa (Fig. 8). This value exceeds the stated yield strength of 250 MPa and, together with local factor-of-safety values below unity, indicates a risk of local yielding and premature fatigue failure under the 100 MPa loading case.

Fig. 9 presents the equivalent elastic strain distribution. Its spatial pattern is consistent with the stress field and identifies the highly strained contact regions.

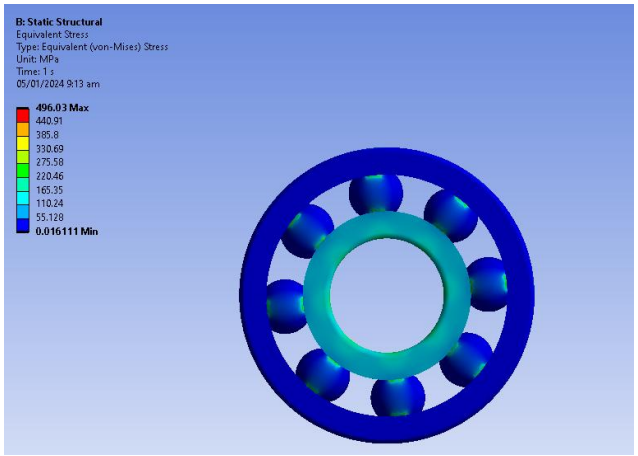

Fig. 8. Von Mises Stress Distribution in the Bearing Model

The load path extends from the inner race through the balls to the outer race. High local contact pressure and subsurface shear stress develop at the ball–race contacts and can promote surface-initiated spalling. The ball stress profiles in Fig. 10 show a narrow contact patch and a steep through-depth stress

© Mehran University of Engineering and Technology 2026

gradient, confirming the highly localised nature of the contact and its importance in fatigue initiation.

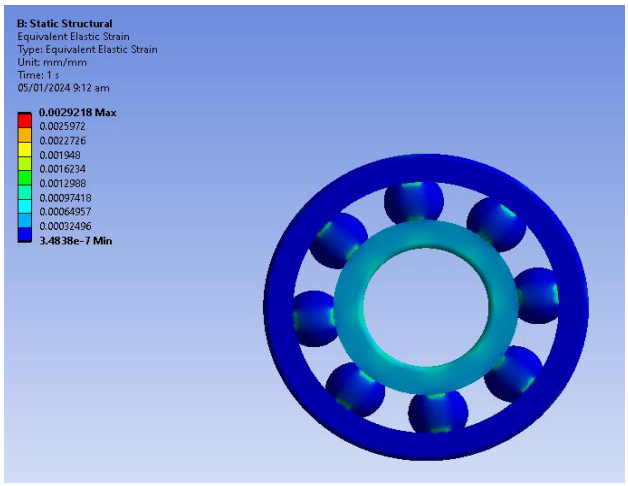

Fig. 9. Equivalent Elastic Strain Distribution in the Bearing Model

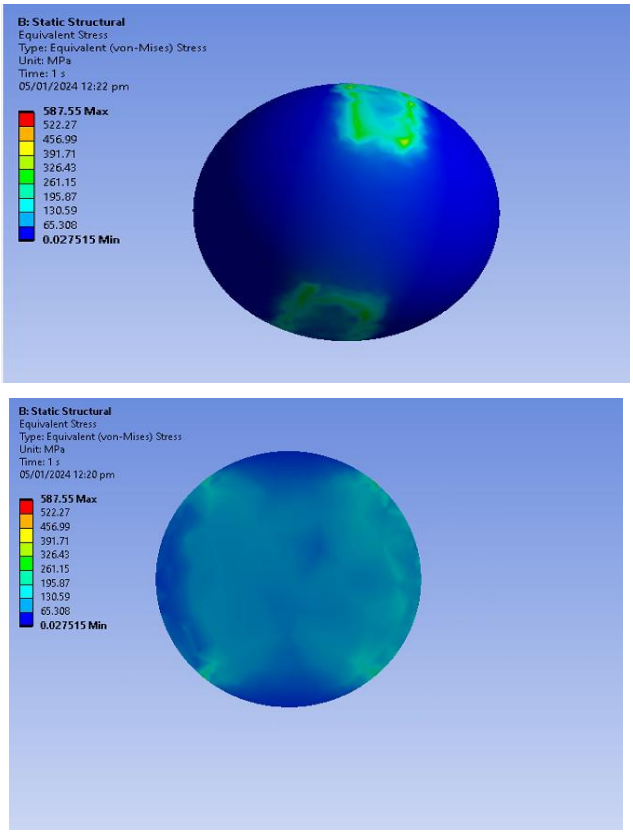

Fig. 10. Stress Profiles of the Ball Bearing

4.2 Fatigue Analysis and Life Prediction

The Goodman criterion was used to evaluate fatigue performance. Fig. 12 shows the reversed load cycle simulated in ANSYS APDL. Under the 100 MPa load, local factor-of-safety values fell below 1.0, indicating a high risk of premature fatigue failure. Predicted fatigue life varied substantially across the bearing, from 1,473 to 1 × 10^6 cycles.

When the applied pressure was reduced to 10 MPa, the minimum factor of safety increased to 1.73 (Fig. 15), and the minimum predicted fatigue life reached 1 × 10^6 cycles. This improvement demonstrates the strong sensitivity of bearing life to operating load and the usefulness of the model for design optimisation.

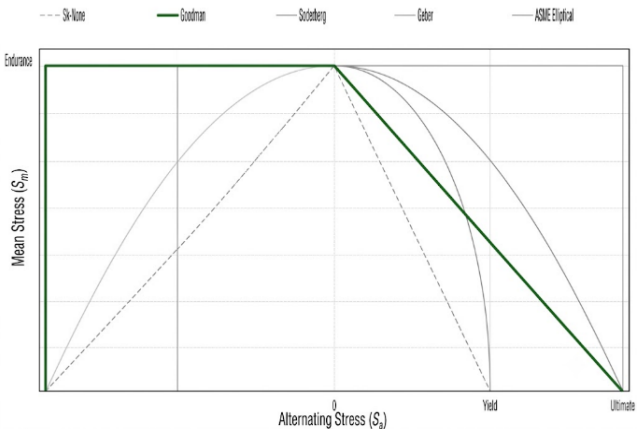

Fig. 11. Comparison of Mean-Stress Theories

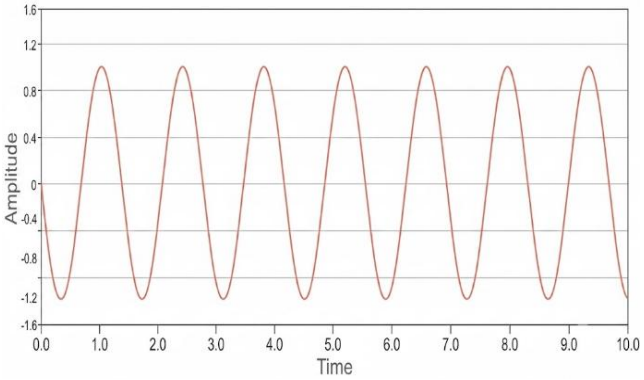

Fig. 12. Reversible Loading of the Ball Bearing

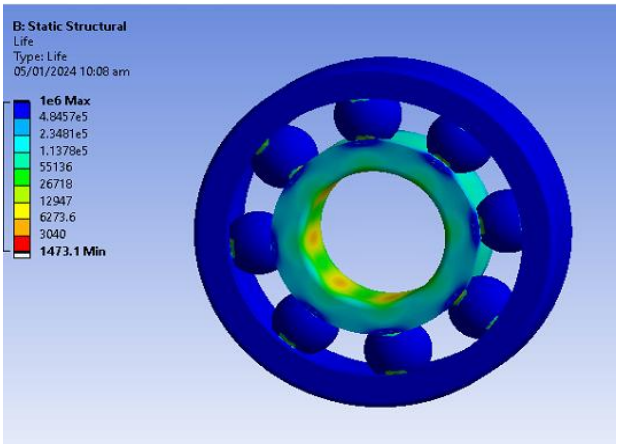

Fig. 13. Bearing Life at 100 MPa Under Reversed Loading

4.3 Comparison of Goodman and Soderberg Fatigue Criteria

To provide a comparative assessment, the Soderberg fatigue criterion was applied to the same finite element model and loading conditions. This criterion is more conservative than the Goodman criterion because it uses the yield strength σ_y rather than the ultimate tensile strength σ_u as the mean-stress reference. Its formulation is:

$$\sigma_a/\sigma_e + \sigma_m/\sigma_y \leq 1 \qquad (5)$$

© Mehran University of Engineering and Technology 2026

For the structural steel used in this study, the yield strength is σ_y = 250 MPa, and the ultimate tensile strength is σ_u = 460 MPa. Because the Soderberg criterion uses the lower yield strength, it imposes a stricter limit on permissible mean stress and therefore predicts a lower factor of safety than the Goodman criterion for the same stress state.

Both criteria were evaluated at radial pressures of 100 and 10 MPa. The results are summarised in Table 1.

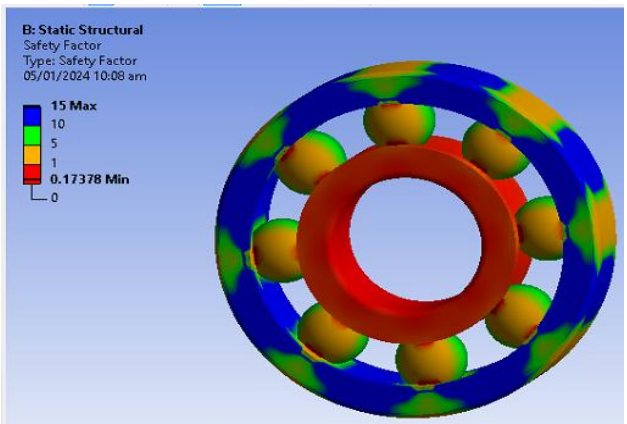

Fig. 14. Bearing Safety Factor at 100 MPa Under Reversed Loading

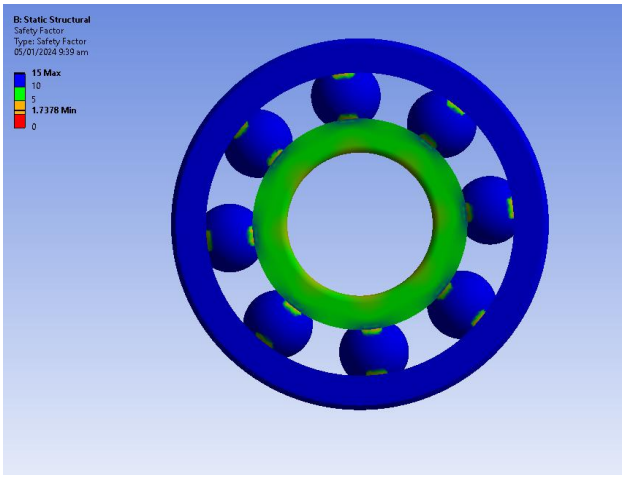

Fig. 15. Bearing Safety Factor at 10 MPa Under Reversed Loading

Table 1

Comparison of Goodman and Soderberg Criteria

Parameter	Goodman (100 MPa)	Soderberg (100 MPa)	10 MPa (Goodman/Soderberg)
Minimum factor of safety	< 1.0	< 1.0	1.73 / ≈1.45
Minimum fatigue life	1,473 cycles	≈900 cycles	1 × 10^6 cycles
Failure risk	High	High	Low

Table 1 shows that both criteria predict unsafe operation at 100 MPa, with minimum factor-of-safety values below unity. The Soderberg criterion predicts a shorter minimum life, approximately 900 cycles, than the Goodman criterion, 1,473 cycles, reflecting its greater conservatism. At 10 MPa, the minimum factor-of-safety values are 1.73 for Goodman and approximately 1.45 for Soderberg; both exceed unity and indicate operation within the endurance limit. The lower Soderberg value illustrates the importance of criterion selection for safety-critical bearings. Goodman provides a practical balance for general engineering design, whereas Soderberg is appropriate when larger safety margins are required or when loading is uncertain.

Conclusion

This study developed and evaluated an integrated finite element method framework for contact-stress analysis and fatigue-life prediction of a deep-groove ball bearing. The Goodman and Soderberg mean-stress criteria were implemented within the same simulation environment to provide a comparative assessment of bearing integrity under realistic loading scenarios.

The framework combines refined mesh generation at critical contact interfaces, realistic contact definitions, and systematic post-processing to produce spatial maps of stress, fatigue life, and factor of safety. These maps identify high-risk regions within the bearing and support design and maintenance decisions.

The analysis predicted a maximum von Mises stress of approximately 496 MPa under a radial pressure of 100 MPa, while both the Goodman and Soderberg analyses produced local factor-of-safety values below 1.0, indicating a high risk of premature failure. Reducing the pressure to 10 MPa substantially improved fatigue performance: the minimum factor of safety was 1.73 with Goodman and approximately 1.45 with Soderberg, and the predicted life reached 1 × 10^6 cycles. The Soderberg criterion consistently produced lower safety factors and shorter life estimates because it uses yield strength rather than ultimate tensile strength as the mean-stress reference. It is therefore suitable for conservative, safety-critical design, whereas Goodman offers a practical balance between accuracy and simplicity for general applications. Future work should incorporate speed-dependent, time-varying loading, elastohydrodynamic lubrication, and thermomechanical coupling. Experimental validation using strain gauges, photoelasticity, or Hertzian analytical benchmarks

© Mehran University of Engineering and Technology 2026

would further improve fatigue-limit estimation and support advanced multiaxial fatigue models.

References

[1] S. Bhatti, A. A. Shaikh, A. Mansoor, and M. Hussain, "New approaches of stochastic models to examine the vibration features in roller bearings," Appl. Sci., vol. 14, Art. no. 1616, 2024, doi: 10.3390/app14041616.

[2] S. Bhatti, A. A. Shaikh, A. Mansoor, and R. Shaikh, "Extraction and classification of vibration features of rolling-element bearings with increasing rotational speed," Mehran Univ. Res. J. Eng. Technol., vol. 43, no. 4, pp. 182–191, 2024.

[3] S. Bhatti, A. A. Shaikh, A. Mansoor, and W. A. Shaikh, "Investigation of faults in a rotating machine using vibration techniques," Sindh Univ. Res. J. (Sci. Ser.), vol. 53, no. 3, pp. 257–264, 2021.

[4] K. L. Johnson, Contact Mechanics. Cambridge, UK: Cambridge University Press, 1985.

[5] T. A. Harris and M. N. Kotzalas, Rolling Bearing Analysis, 5th ed. Boca Raton, FL, USA: CRC Press, 2006.

[6] P. Gupta, Advanced Dynamics of Rolling Elements. Berlin, Germany: Springer, 2011.

[7] Kapoor and R. Sadeghi, "Finite element analysis of rolling contact in bearings," Tribol. Int., vol. 41, no. 8, pp. 740–748, 2008.

[8] Y. Liu, J. Wang, and J. Zhou, "Dynamic contact analysis of deep-groove ball bearings under time-varying loads," Mech. Mach. Theory, vol. 129, pp. 1–14, 2018.

[9] S. Li and M. Motooka, "A finite element method used for contact analysis of rolling bearings," Shimane University, 2023.

[10] Dassault Systèmes, SolidWorks Simulation, 2021.

[11] Y. Guo and R. G. Parker, "Stiffness matrix calculation of rolling-element bearings," Mech. Mach. Theory, 2012.

[12] T. A. Harris and M. N. Kotzalas, Rolling Bearing Analysis, 5th ed. CRC Press.

[13] ANSYS Inc., ANSYS Mechanical 2021 R2 User Manual, 2021.

[14] J. Goodman, Mechanics Applied to Engineering. London, UK: Longmans, Green and Co., 1899.

© Mehran University of Engineering and Technology 2026